



**ISLAMIC UNIVERSITY OF TECHNOLOGY**  
**ORGANISATION OF ISLAMIC COOPERATION**



**NUMERICAL INVESTIGATION OF LOCAL SCOUR  
AROUND DIFFERENT SHAPED BRIDGE PIERS USING  
FLOW-3D SOFTWARE**

B.Sc. Engineering (Mechanical) Thesis

**Authored by  
Md Abid Shahriyar**

**St Id: 151453**

**SUPERVISED BY**

**PROF. DR. MD. HAMIDUR RAHMAN**

Department of Mechanical and Production Engineering (MPE),  
Islamic University of Technology (IUT)

**DEPARTMENT OF MECHANICAL AND PRODUCTION ENGINEERING  
(MPE)**

**Islamic University of Technology (IUT)**

**March, 2021**

## CERTIFICATE OF RESEARCH

This thesis titled "NUMERICAL INVESTIGATION OF LOCAL SCOUR AROUND DIFFERENT SHAPED BRIDGE PIERS USING FLOW-3D SOFTWARE" submitted by Md Abid Shahriyar (151453) has been accepted as satisfactory in partial fulfillment of the requirement for the Degree of Bachelor of Science in Mechanical Engineering.

Supervisor



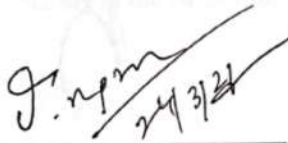
---

**PROF. DR. MD. HAMIDUR RAHMAN**

Department of Mechanical and Production Engineering (MPE)

Islamic University of Technology (IUT)

**Head of the Department**



---

**PROF. DR. MD. Anayet Ullah Patwari**

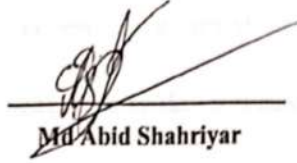
Department of Mechanical and Production Engineering (MPE)

Islamic University of Technology (IUT)

**Candidate's Declaration**

It is hereby declared that, my thesis or any part of it has not been submitted elsewhere for the award of any degree or diploma.

**Signature of the Candidate's**



**Md Abid Shahriyar**

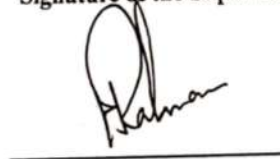
**Student ID: 151453**

Department of Mechanical and Production Engineering (MPE)

Islamic University of Technology (IUT) Board Bazar

Gazipur-1704, Dhaka, Bangladesh

**Signature of the Supervisor**



**PROF. DR. MD. HAMIDUR RAHMAN**

Department of Mechanical and Production Engineering (MPE)

Islamic University of Technology (IUT)

## **Acknowledgments**

I would like to express my sincere thanks to our respected supervisor Prof. Dr. Md. Hamidur Rahman sir for his continuous support and guidance throughout this research period and my undergraduate study. His motivation and advice helped me a lot in every step of this research work and writing of this thesis book. His constructive comments helped me a lot to understand and complete this research work.

I am also grateful to my beloved parents for their continuous encouragement and support.

## Table of contents

Abstract .....	10
Chapter 1 Introduction.....	11
Chapter 2 Literature Review.....	13
Basic theory related to scouring.....	13
Scour and its classification .....	14
Scouring mechanism .....	15
Factors affecting bridge scour .....	16
Chapter 3 Numerical Methodology .....	18
Governing equations .....	18
Bed shear stress.....	18
Critical shields parameter .....	19
Entrainment and deposition .....	19
Bed load transport .....	19
Suspended load transport.....	18
Turbulence modelling .....	18
Numerical modelling of bed.....	20
Grid test .....	21
Chapter 4 Result Analysis.....	26
Comparison of numerical and experimental bed topography at equilibrium .....	28
The circular shaped pier.....	29
The square shaped pier .....	29
The diamond shaped pier.....	29
The hexagonal shaped pier .....	29
The airfoil shaped pier.....	29
Validation of scour depth when the time is varied .....	29

The circular shaped pier .....	30
The square shaped pier .....	30
The diamond shaped pier.....	31
The hexagonal shaped pier .....	32
The airfoil shaped pier.....	32
Velocity distribution along the flume bed.....	32
Chapter 5 Summary and Conclusions.....	33
References.....	38

#### List of Figures

Figure 1: Scouring effect around a bridge pier.....	11
Figure 2: Bridge failure due to scouring effect both (a) & (b).....	12
Figure 3: Shield diagram/curve .....	14
Figure 4: Classification of scour.....	15
Figure 5: Scouring mechanism due to horse shoe vortex system(THSV) .....	16
Figure 6: Horse shoe and wake vortices around a cylindrical element .....	16
Figure 7: Circular bridge pier geometry .....	21
Figure 8: Square bridge pier geometry .....	21
Figure 9: Diamond bridge pier geometry.....	21
Figure 10: Hexagonal bridge pier geometry .....	22
Figure 11: Airfoil bridge pier geometry .....	21
Figure 12: Location of mesh plane at $x= 3.5\text{m}$ and $x=4.5\text{m}$ from inlet.....	22
Figure 13: Boundary conditions .....	22
Figure 14: Meshing of geometry .....	22
Figure 15: Grid refinement around bridge piers.....	22
Figure 16: Grid independency test.....	22
Figure 17: Comparison of experimental (bottom) and numerical (top) bed topography at equilibrium (in cm) for circular shaped pier.....	24
Figure 18: Comparison of experimental (bottom) and numerical (top) bed topography at equilibrium (in cm) for square shaped pier .....	25
Figure 19: Comparison of experimental (bottom) and numerical (top) bed topography at equilibrium (in cm) for diamond shaped pier .....	25
Figure 20: Comparison of experimental (bottom) and numerical (top) bed topography at equilibrium (in cm) for hexagonal shaped pier.....	26

Figure 21: Comparison of experimental (bottom) and numerical (top) bed topography at equilibrium (in cm) for airfoil pier.....	26
Figure 22 : scouring depth at equilibrium condition in 3D geometry (a) circular pier (b) square pier and (c) diamond pier .....	28
Figure 23: scouring depth at equilibrium condition in 3D geometry (d) hexagonal .....	28
Figure 24: change of maximum scour depth(cm) with time(sec) for both experimental and numerical case for circular pier .....	29
Figure 25: change of maximum scour depth(cm) with time(sec) for both experimental and numerical case for square pier.....	29
Figure 26: change of maximum scour depth(cm) with time(sec) for both experimental and numerical case for diamond pier .....	29
Figure 27: change of maximum scour depth(cm) with time(sec) for both experimental and numerical case for hexagonal pier .....	30
Figure 28: change of maximum scour depth(cm) with time(sec) for both experimental and numerical case for airfoil pier.....	30
Figure 29: Without collar scouring depth and velocity profile.....	31
Figure 30: Reduction of scouring after adding collar and velocity profile.....	32
Figure 31: Comparison of numerical maximum scour depth(cm) among five piers structures.....	33
Figure 32: Comparison of numerical maximum scour height(cm) among five piers structures.....	34
Figure 33: Comparison among square, diamond, hexagonal and airfoil piers.....	35
Figure 34: (a) circular shaped bridge piers with one collar around pier and (b) circular shaped bridge piers with two collars around pier.....	35

## List of Tables

Table 1: Pier geometry and bed structure data and location of pier from inlet.....	21
Table 2: Sand properties and used turbulent model .....	21
Table 3: Number of grid nodes in each direction and number of total cells in each grid system.....	22
Table 4: Numerical and experimental maximum scour depth(cm) for circular, square and diamond pier .....	34
Table 5: Comparison between experimental and numerical result for maximum scour depth.....	34
Table 6: Numerical and experimental maximum deposition height(cm) for circular, square and diamond pier .....	34
Table 7: Numerical maximum scour depth(cm) and maximum deposition height(cm) for hexagonal and airfoil pier.....	34



## Nomenclature

$\tau_o$  = bed shear stress(Pa)

$\tau_c$  = critical shear stress(Pa)

$R_{*c}$  = Shear Reynolds number

$\tau_{*c}$  = Non-dimensional shear stress

$u_{*c}$  = shear velocity at the critical condition (m/s)

$\Upsilon$  = unit weight of water(N/m<sup>3</sup>)

$\Upsilon_s$  = unit weight of sediment

particle(N/m<sup>3</sup>)  $\nu$  = kinematic viscosity

of water (Ns/m<sup>2</sup>)

$d_{50}$  = mean diameter of sand particle(mm)

$\Theta_n$  = critical shield parameter

$g$  = acceleration of

gravity(m<sup>2</sup>/s)  $\rho$  = density of

water(kg/m<sup>3</sup>)

$\rho_s$  = density of sand(kg/m<sup>3</sup>)

$d^*$ , = dimensionless grain size

$\Phi_n$  = dimensionless bed load transport parameter

$B_n$  = the bed load coefficient

$C_s$ , = suspended sediment mass

concentration  $t$  = time(sec)

## Abstract

Scour is a natural event caused by the erosive action of flowing water on the bed and banks of streams, which also takes place on region in the vicinity of the bridge piers and abutments. In this analysis I have tried to investigate whether Flow-3d can accurately predict the scouring geometry, the depth and deposition of sand around bridge piers or not. In this study mainly the scouring in case of non-cohesive bed sediment was simulated using the software where both the qualitative and quantitative analysis have been presented. And the software uses Reynold's Average Navier Stokes (RANS) equation closed with k- $\epsilon$  model with second order accurate turbulence method. The study gives a conclusion which suggest that among the different five shapes (circular, square, diamond, hexagonal, airfoil), for circular shape the scour depth is satisfactory than other diamond and hexagonal shape but in case of airfoil scouring is so high that it didn't catch our thought anyway. Besides these, it also shows that scouring is higher in the upstream of the piers than the downstream. Another major finding of my work is that there are some limitations in the Flow-3d software to predict the scouring depth. The two major countermeasure techniques employed for preventing or minimizing local scour around bridge piers are: (i) bed armoring countermeasures and (ii) Flow-altering methods. I have introduced a collar around circular shaped piers to see whether scouring depth is decreased or not.

**Keywords:** *local scour, horseshoe vortex system (THSV), scour depth, bed topography, CFD, non-cohesive sand, deposition height, critical shields number.*

## Chapter 1 Introduction

Scouring is a very general and common phenomena which occurs in the rivers or other streams and causing the breakdown and failures of many bridges of the world. The study on scouring is developing day by day and it can't be fully removed rather the measure of erosion and bridge failure can be reduced with the help of adapting some measures. Local scour occurs due to the heavy pressure flow on the upstream of the riverside which creates horse shoe vortex around the sets of piers and by the influence of the pillars and high shear stress the underneath sands are moving from the region and creates an area where the supportive non cohesive soil is not present causing the bridge to fail. And extensive work around the world is going on to reduce the failures of bridges. Flood or the increased water flow which at the same time increases the pressure on the structure causes the downward movement of the sand layer around bridge levels and some areas around the pillars of the bridges. Formation of scour pit for flooded condition is playing a vital role in the erosion process.



*Figure 1: Scouring effect around a bridge pier[16]*



*Figure 2: Bridge failure due to scouring effect*

In the field of scouring many researchers have studied the various aspects of local scour like temporal and equilibrium scour (Melville and Chiew 1999[31], Kothiyari et al 1992a[32], Johnson and Bilal 1992[33], Laursen 1963[34]), clear water and live bed scour (Vittal et al 1994[35], Jain 1981[36], Kothiyari et al 1992b[37], Laursen 1962[38]), scour in uniform and non-uniform bed materials (Melville and Chiew 1999[31], Molinas and Abdeldayem 1998[39], Raudkivi and Ettema 1977[40]), scale effects in pier scour (Kabir et al 2000[41], Laursen 1963[34], Laursen 1962[38]) and so on. Again many empirical equations (Kandasamy and Melville 1998[42], Melville and Sutherland 1988[43], Poona (Chang 1988[44], Garde and Raju 1985[45]) and mathematical models (Ram 1999[30], Johnson and Bilal 1996[46], Dey et al 1995[47]) are available for predicting pier scour depth, which are usually intended to estimate the ultimate scour depth. More recently attempts were made to reduce scour with the piers of different shape, geometry and orientation (Sheppard and Jones 1998[48], Kumar et al 1999[49], Parola 1996[50], Lim and Chiew 1999[51]).

Thus the main objectives of our study is to investigate the scouring effect for different shapes of the pillar structures like circular, square, diamond, hexagonal and airfoil and to do a comparative analysis between these structures to find a conclusion of which one is better in implementing as pillar structure.

In summary it mainly discussed the scour evolution under the flooded bridge piers for different structures and this study has been done based on computational fluid dynamics using FLOW -3D which can predict the scouring more precisely.

## Chapter 2 Literature Review

### 2.1 Basic theory related to scouring:

The alluvium or sediment refers to the loose and non-cohesive element which usually move due to the action of water with varying velocity and resulting deposition or transportation of it. And the initiation of the motion of the sediment depends upon the bed shear stress which can be defined as

$$\tau_o = \gamma R S_o \quad [22] \dots \dots \dots (1)$$

These two numbers are Shear Reynolds number and non-dimensional shear stress [22] which can be expressed in equation like

$$R_{*c} = \frac{u_{*c} d}{\nu} \quad (\text{Shear Reynolds number}) \dots \dots \dots (2)$$

$$\tau_{*c} = \frac{\tau_c}{(\gamma_s - \gamma)d} \quad (\text{Non-dimensional shear stress}) \dots (3)$$

Where,  $d$  = diameter of the bed particle

$\gamma_s = \rho_s g$  = unit weight of the sediment particle

$\gamma = \rho g$  = unit weight of water

$\tau_c$  = critical shear stress

$u_{*c} = \sqrt{\frac{\tau_c}{\rho}}$  = shear velocity at the critical condition

$\nu$  = kinematic viscosity of water

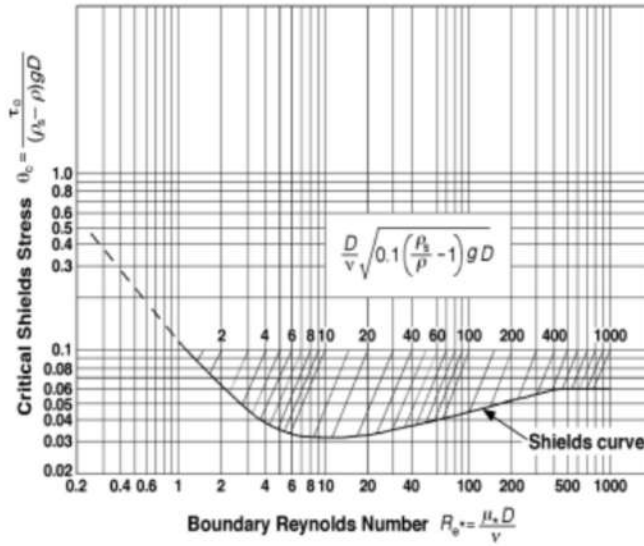


Figure 3: Shield diagram/curve[22]

From the Shields curve it is very clear that up to  $R_{*c} = 2$  the flow is pretty much smooth in nature and particle diameter doesn't have any effect on the critical shields stress. For  $2 < R_{*c} < 400$  there has a transition stage and both the velocity and particle diameter has effect on critical shields stress and after that range it became nearly constant. As the size of the sediment is non uniform in nature so it is convenient to take median size ( $d_{50}$ ).

## 2.2 Scour and its classification:

It is a general phenomenon occurs due to the flow of water where sediment is being moved. Scour generally influences by the effects of abutments and piers when water passes across these structures and a net change in the bed elevation is observed. When the bed elevation decreases due to the erosion of bed then it is called as degradation where the increase of bed elevation due to the deposition of sediment is called as aggradation. Scouring can be divided into three main types which are:





Figure 4: Classification of scour

- i. **Degradation Scour:** The long-term process which causes the lowering of the sediment bed for the flow of water and which is may not be evident after passing of the flood event.
- ii. **Contraction Scour:** Which occurs due to the contraction of the flow passage area of the water naturally or due to other obstructions and result increasing velocity in the water flow. It is commonly termed as general scour.
- iii. **Local Scour:** This type of scour happening due to the abutments and piers which create vortex around the hydrodynamic structure and take the sediment away from the structure making it very weak and unsafe.

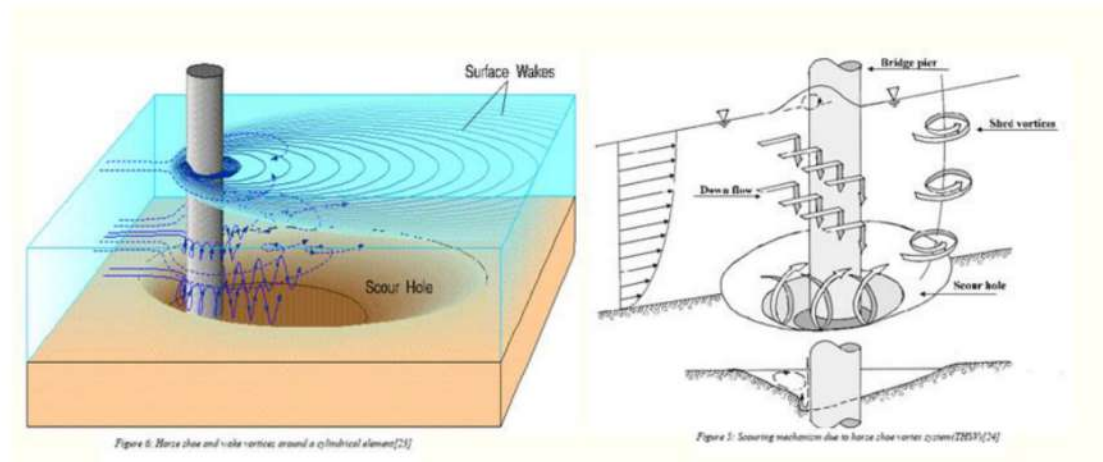
*Local scour are two types:*

- a) **Clear-water Scour:** It refers to the condition where there is no sediment movement thus no sediment is being transported to the scour prone zone due to this type of scour.
- b) **Live-bed Scour:** Here sediment is transported with water in the flowing direction and which led the decrease in the height of the scour.

### 2.3 Scouring mechanism:

The maximum failures of bridges occur for the scouring which removes the sediment from the base of piers. And research are being carried out across the world to make the pier design safe

and economical. When water is flowing toward the pier there creates a stagnation point at the intersection between the pier and the direction of the flow where velocity comes to complete rest. The velocity distribution of the approaching flow varies from zero at the bed surface up to the maximum at the surface of water that creates a pressure gradient from the bottom pier to the top. This change in pressure creates vortex at the bottom of the pillar that sweeps sediment from the region and the vortex looks like a horseshoe. For that reason, this type of vortex is called horseshoe vortex. Horseshoe vortex mechanism can be illustrated with figure 5 and 6.



## 2.4 Factors affecting bridge scour:

Local scour and General scour are very much affected by some important factors and these factors has been discussed by (Melville and Coleman, 2000)[24]

**Flow parameters:** Which include the approach flow velocity, the angle of contact between the flowing fluid and the structural geometry. **Fluid property:** The property of any fluid has been characterized by its density ( $\rho$ ) and viscosity ( $\nu$ ). And these parameters are sensitive to the temperature change. **Geometrical factors:** Shape and structure of the pier has an imperative impact on the scouring issue. **Time:** Reaching into equilibrium condition there need some time and enough time should be provided for equilibrium condition to be exist. particle size,distribution for non-cohesive sediments, spatial distribution of sediment size are important factors. As you can see, we have taken



4m downstream for pillar location. There has a number of way of turbulence modelling and in this analysis we have used Renormalized Group(RNG) turbulence modelling which is the simplest and the most effective method of establishing scaling of specific models and calculating the corresponding critical exponents.

### 3. NUMERICAL METHODOLOGY

#### 3.1 Governing equations:

In this work FLOW-3D has been used for simulation purpose. Where it has been fully coupled with fluid flow, allows multiple non-cohesive species and considers entrainment, deposition, bed load transport and suspended load transport. Volume and area fraction that describe the packed sediment are calculated throughout the whole domain at each and every time step that is being incorporated by the user.

The equations that have been used are given below:

##### 3.1.1 Bed shear stress:

$$u = u_\tau \left[ \frac{1}{K} \ln \left( \frac{Y}{u_\tau + k_s} \right) \right] \quad [25] \quad \dots \dots \dots (4)$$

Where,  $u_\tau$  = the shear velocity,  $u_\tau = \sqrt{\frac{\tau}{\rho}}$ ,  $\tau$  = bed shear stress and  $\rho$  = bulk density of the fluid-sediment mixture,

$Y$  = distance from the wall,

$\nu$  = kinematic viscosity of the bulk flow,

$K = 0.4$  is the Von Karman Constant and  $k_s$  is related to the grain size and can be defined as

$$k_s = C_s d_{50} \dots \dots \dots (5)$$

$d_{50}$  = Median grain diameter of the bed material,

$C_s$  = user defined coefficient, usually recommended value is 2.5.

##### 3.1.2 Critical shields parameter:

$$\Theta_n = \frac{\tau}{g d_n (\rho_n - \rho_f)} \dots \dots \dots (6)$$

$$\Theta_{cr,n} = \frac{\tau_{cr,n}}{g d_n (\rho_n - \rho_f)} \dots \dots \dots (7)$$

$$\Theta_{cr,n} = \frac{0.3}{1+1.2 d_{*,n}} + 0.055(1 - e^{-0.02 d_{*,n}}) \dots (8)$$

$$d_{*,n} = d_n \left[ \frac{g(S_n-1)}{\nu_f^2} \right] \dots (9)$$

### 3.1.3 Entrainment and deposition:

$$u_{lift,n} = n_b \alpha_n d_{*,n}^{0.3} (\Theta_n - \Theta_{cr,n})^{1.5} \sqrt{g d_n (S_n - 1)} \dots (10)$$

$$u_{settle,n} = \frac{g}{g} \left[ (10.36^2 + 10.49 d_{*,n}^3)^{\frac{1}{2}} - 10.36 \right]^{\frac{\nu_f}{d_n}} \dots (11)$$

### 3.1.4 Bed load transport:

$$\Phi_n = \frac{q_{b,n}}{[g(S_n-1)d_n^3]^{\frac{1}{2}}} \dots (12)$$

$$\Phi_n = B_n (\Theta_n - \Theta_{cr,n})^{1.5} C_{b,n} \dots (13)$$

$$C_{b,n} = \frac{\text{net volume of } n \text{ species}}{\text{net volume of all species}} \dots (14)$$

$$\sum_{n=1}^N C_{b,n} = 1.0 \dots (15)$$

$$h_n = 0.3 d_n d_{*,n}^{0.7} \left( \frac{\Theta_n}{\Theta_{cr,n}} - 1 \right)^{0.5} \dots (16)$$

$$u_{b,n} = \frac{q_{b,n}}{h_n C_{b,n} \rho_b} \dots (17)$$

### 3.1.5 Suspended load transport:

$$\frac{\partial C_{s,n}}{\partial t} + \nabla \cdot (C_{s,n} u_{s,n}) = \nabla \cdot \nabla (D C_{s,n}) \dots (18)$$

$$C_{s,n} = \frac{c_{s,n}}{\rho_n} \dots (19)$$

$$\bar{\rho} = \sum_{m=1}^N c_{s,m} \rho_{s,m} + (1 - c_{s,tot}) \rho_f \dots (20)$$

$$c_{s,tot} = \sum_{m=1}^N c_{s,m} \dots (21)$$

### 3.2 Turbulence modelling:

There has a number of way of turbulence modelling and in this analysis we have used Renormalized Group (RNG) turbulence modelling which is the simplest and the most effective

method of establishing scaling of specific models and calculating the corresponding critical exponents. The Renormalized Group (RNG)  $k-\epsilon$  model (Yakhot & Orszag 1986, Yakhot & Smith 1992) is a more robust version of the two-equation  $k-\epsilon$  model, and is suggested for most industrial problems.

The Yakhot-Orszag renormalization group has been developed to solve non-linear turbulence equations and that has been done by evaluation of Reynolds stresses of second order in the  $\epsilon$  expansion of the Yakhot-Orszag theory. And because of its converging nature for different turbulent models it has been used for the analysis of scouring process in this paper.

### **3.3 Numerical modelling of bed:**

In this analysis we have numerically studied on the turbulent flow over the open channel bed with a vertical pillar mounted on the bed and which has been located 4m downstream of the inlet region of water flow. This study has been dealt with a total number of five geometric structures of pillars which are a circular pier, square shaped pier, diamond shaped pier, hexagonal shaped pier(new case study) and an airfoil shaped pier(new case study). These piers are shown in figure 7,8,9,10 and 11.

In the case of circular pier, the diameter has been taken as 16.51 cm. For square shaped pier, each edge length is 16.51cm and for diamond shaped pier, width is 23.35 cm. The related dimension of circular, square and diamond piers are taken from the experiment of Ali Khosronejad&Seokkoo (2012)[26]. Considering the hydraulic diameter of previous three shapes, we determined the edge length of 10 cm for hexagonal shape. The distance between two edge is 50 cm (around 3 times of diameter) & diameter is 17 cm for the airfoil one. The total length of the bed is 10m long and has a rectangular cross-section which is 1.21m wide and 45cm deep. And the flume has a 20 cm layer of uniformly graded non-cohesive sand with a mean particle diameter of  $d_{50} = 0.85mm$ [26].

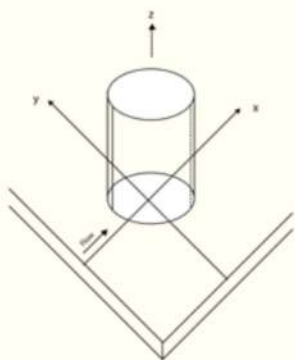


Fig 7: Circular pier

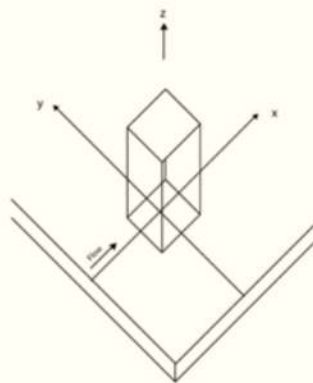


Fig 8: Square Pier

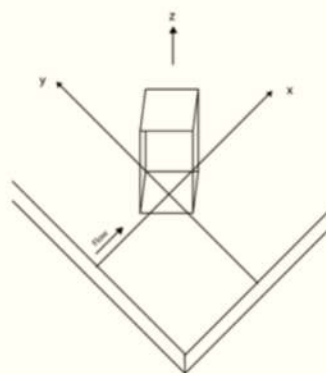


Fig 9: Diamond Pier

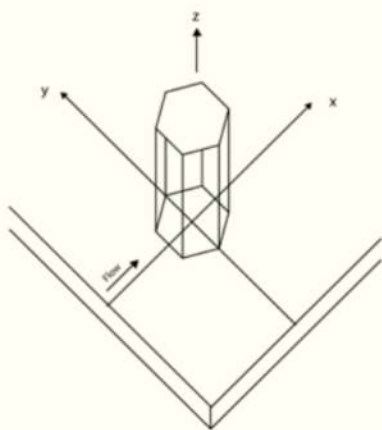


Fig 10: Hexagonal Pier

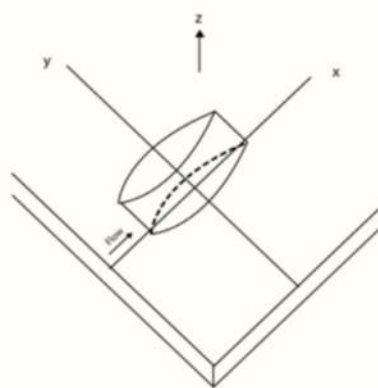


Fig 11: Aerofoil Pier

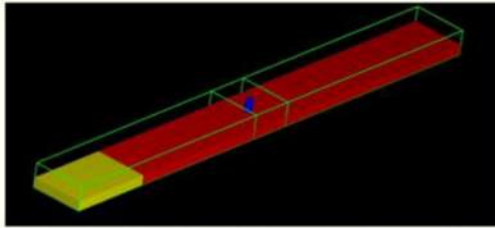


Fig12: Location of mesh plane at x=3m & x=5m

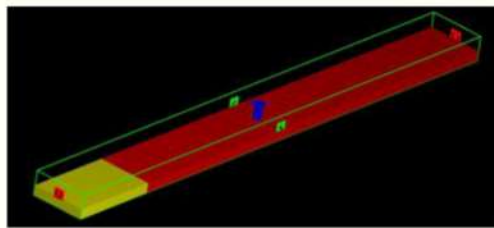


Fig13: Boundary condition

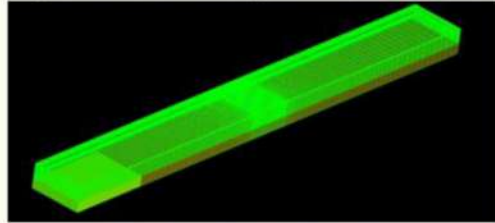


Fig14: Meshing of geometry

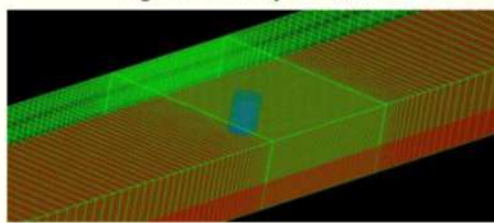


Fig15: Grid refinement around bridge piers

### 3.4 Grid test:

Grid independency has been carried out in case of circular pier. Where the rectangular structured mesh are ranging over the sediment bed and the pillar. A number of cells has been defined to discretize the governing equations. The resolution of the grid has changed from the coarser one to the finer one to get acquainted with the effect of structured grid over the numerical result. FLOW-3D is dealing with the structured rectangular mesh and for that reason it is implemented on our overall structure.

Grid	Number of grid nodes	Total number of cells
A	333 × 30 × 20	200000
B	166 × 50 × 30	250000
C	200 × 50 × 30	300000

Table 1: Number of grid nodes in each direction and number of total cells in each grid system

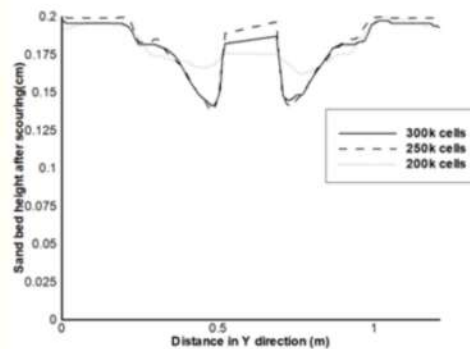


Fig16: Grid independency test

The above graph illustrates that A (coarsest) with total 200k number of cells cannot predict the scour depth accurately where the results of scour depth for B (with 250k) and C (with 300k) are very close to each other which confirms that grid independency is achieved. So the finest grid C has been taken as a prime one to run the rest of the simulations for other structures. For all these cases time accurate simulations were carried out until it reaches in equilibrium condition.

## 4. RESULT ANALYSIS

### 4.1 Comparison of numerical and experimental bed topography at equilibrium:

In the below, numerical topographies of the three geometrical structures e.g. circular, square and diamond shaped piers have been validated with the experimental data available in Ali Khosronejad & Seokkoo (2012) [26]. All negative contour values represent scouring and positive values represent deposition. All numerical values are in cm unit.

#### 4.1.1 The circular shaped pier:

The maximum scour depth that has been observed for the experimental one is 6.7cm [26] and for the numerical one it is 6.5cm. And both of these results are observed in two different locations where the numerical values for both of the scour depth can be compared with some sacrifice in accuracy.



Figure 17: Comparison of experimental (bottom) and numerical (top) bed topography at equilibrium (in cm) for circular shaped pier

#### 4.1.2 The square shaped pier:

The maximum experimental scour depth has been recorded as 7.6cm [26] and the numerical scour depth is 6.6cm. The difference between the numerical and the experimental results are not satisfactory enough. Because in the real case, scouring around square shaped pier has also been



influenced by the edges of the pier and that accelerate the scouring mechanism and scouring depth increases but the effect of the edges cannot be predicted by the Flow3d software. And for that the scouring depth for those two cases varies a lot.

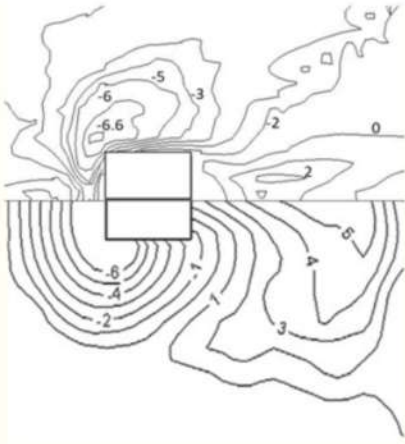


Fig 18 Square shaped pier



Fig 19: Diamond shaped pier

#### 4.1.3 The diamond shaped pier:

Maximum scour depth in the experimental case is 8.3cm [26] and the numerical one is the 8.5cm. So these two values can be compared very easily and here we get a better result.

From the above analysis we can concluded that for both the bed topography and numerical values the predictive capabilities of the CFD software depends on the structure of the pier. And in case of the blunt nose the bed topography is not much satisfactory. But for the diamond shape it has a better predictive ability.

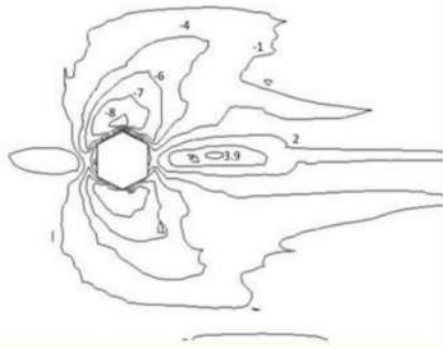


Fig: Hexagonal Shaped pier

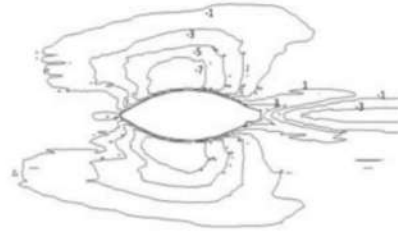


Figure 21: Comparison of experimental (bottom) and numerical (top) bed topography at equilibrium (in cm) for airfoil pier

#### 4.1.4 The hexagonal shaped pier:

Here we see that maximum scour develops at the side of the pillar and gradually decreases when we go far from the pillar center (figure 18). And deposition starts to build up in the downstream of the pier. The maximum scour depth for the numerical one is recorded as 8.0cm and deposition of sand is recorded as 3.9cm. Maximum scouring occurs as a small pocket at both sides.

#### 4.1.5 The airfoil shaped pier:

Airfoil shape is one of our interest of study because of its streamlining structure. In this structure, the maximum scour develops at both side of the pillar and forming a confined, comparatively bigger, pocket like structure (figure 19).

The maximum scour depth that has been recorded for the airfoil structure is 7.9 cm and the deposition at the downstream of the pillar is 3.8cm. The scouring gradually decreases from the side of the pillar. And from the maximum scour depth value there has no development of scouring in case of airfoil structure. (can write about no scouring in the nose side)

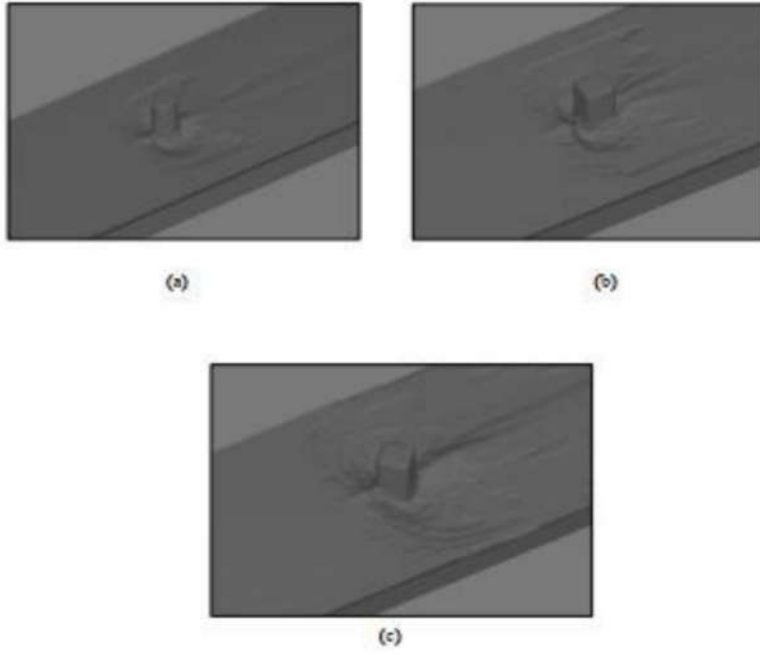
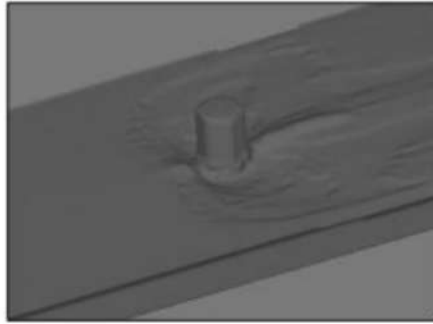
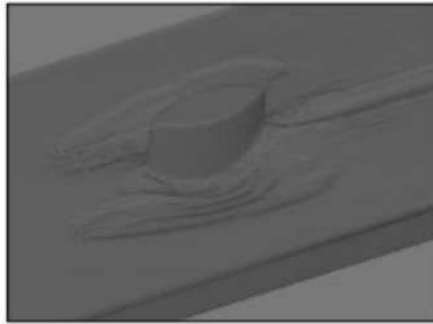


*Figure 22: scouring depth at equilibrium condition in 3D geometry (a) circular pier (b) square pier and (c) diamond pier*



(d)



(e)

*Figure 23: scouring depth at equilibrium condition in 3D geometry (d) hexagonal pier and (e) airfoil pier*

#### **4.2 Validation of scour depth when the time is varied:**

From the mechanism of scouring effect, we know that scouring effect increases with respect to the time. At the starting of a water flow across the pier, the velocity remains quite gentle and which has less effect on the scouring process.

##### **4.2.1 The circular shaped pier:**

In the graph that has been presented below we observe that for the circular shaped pier for the approximately first 300 seconds the shape of the curve of scouring is similar in shape though it has difference in the numerical value.

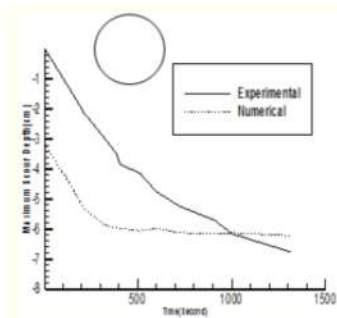


Fig24: Numerical vs. Experimental Scour depth of Circular shaped pier

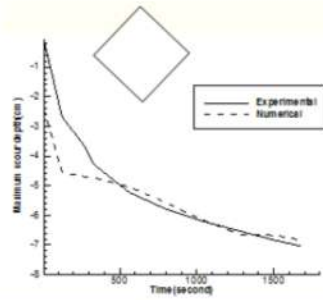


Fig25: Numerical vs. Experimental Scour depth of Diamond shaped pier

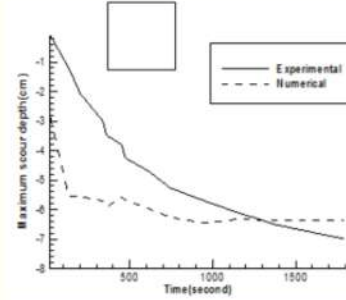


Fig26: Numerical vs. Experimental Scour depth of Square shaped pier

#### 4.2.2 The square shaped pier:

Time dependent analysis of the square shaped pier reflects that the irregularities of scouring depth and corresponding curve is more than the circular shaped pier that we have seen before. And here for the first few seconds though the shape is somewhat similar but not that much. Here also this has happened because of the scouring mechanism which tells us that when the flow started scouring is only driven by the velocity where for the later part horse shoe vortex system is also seen.

#### 4.2.3 The diamond shaped pier:

Diamond shaped pier is one of the topics of interest because of its nature of geometry which has edge shape pier nose when flow is in the upstream. And due to the presence of the edge, the formation of horse shoe vortex ceases. The edge at the upstream decreases the energy of the horse shoe vortex and that subsequently gives us a better result for the diamond shaped pier.

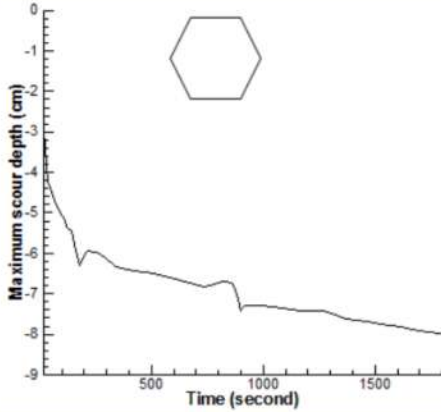


Fig 27: Numerical analysis of time dependent scour depth(Hexagonal shaped pier)

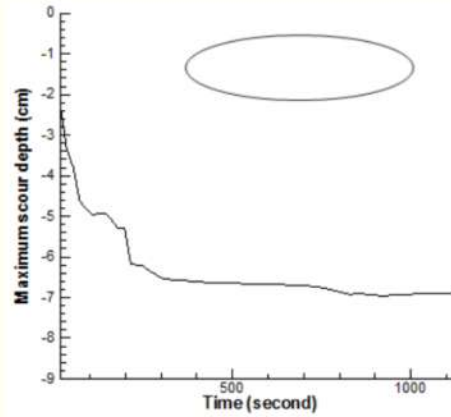


Fig 28: Numerical analysis of time dependent scour depth(Aerofoil shaped pier)

#### 4.2.4 The hexagonal shaped pier:

This is a new case that has been studied by our research. And in light of the graph that has been presented down below we can explain the time dependent nature of scouring effect of the hexagonal shaped pier. According to the graph for the first 200 seconds the rate of scouring is very fast but for the rest of the simulation the rate gradually decreases with time.

#### 4.2.5 The airfoil shaped pier:

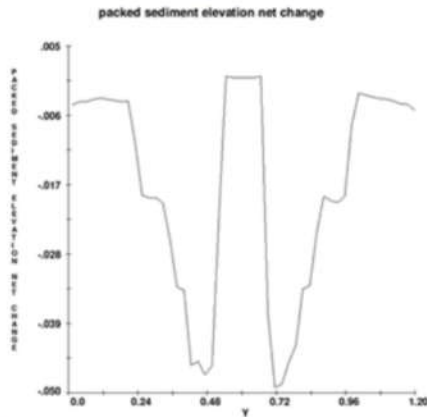
It is another structure that has been newly introduced by our study to see whether it can give a good result or not. We see from the above graph of the airfoil shaped pier that it reached in equilibrium condition very rapidly and at the first phase of the process the rate of scouring is very fast and then suddenly it dropped drastically.

#### 4.3 Velocity distribution along the flume bed:

**Comparison between piers with collar and piers without collar to find desirable scouring depth**



## Without Collar(simulation result)



## Without Collar

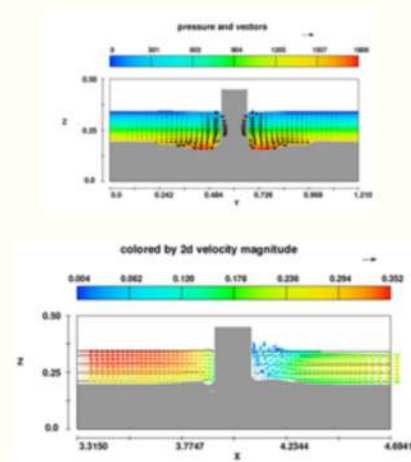
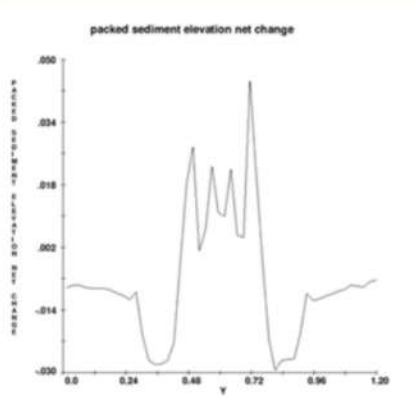


fig 29: Without collar scouring depth and velocity profile

Velocity distribution along the bed flume indicates the theory behind the scouring. Here we see that velocity is not constant along the flume bed rather it is different and follows a pattern. According to the contour plot shown below (fig 29) we acknowledge that velocity is highest at the inlet and that is steadily decreasing and came to a complete stop at the pillar and fluid flow interface. And that point is known as stagnation point and here velocity is very less but at the same time pressure increases. From the contour plot another thing is that velocity is also changing along z direction or vertical plane, which is in the order of decreasing. So there creates a pressure difference along the vertical direction and that pressure gradient influence the scouring process and removes sediment particle from that region. Scouring is higher in the upstream of the flow at the pillar nose. But if we observe the downstream of the pillar then we see that velocity is lowest at the back of the pillar which subsequently creates a region of unsteady flow and eddy formation of water that is irregular. This region in the downstream of the pillar is called wake region and here wake vortex also form. That creates a scouring region behind the pillar. As the velocity is very negligible at that region so formation of scour depth is also very small. And beyond the wake region flow again starts to accelerate. Though no scouring is not observed further because there is no abutments or pillar on their flow which could create an obstacle and form local scour.

With Collar(simulation result)



With Collar

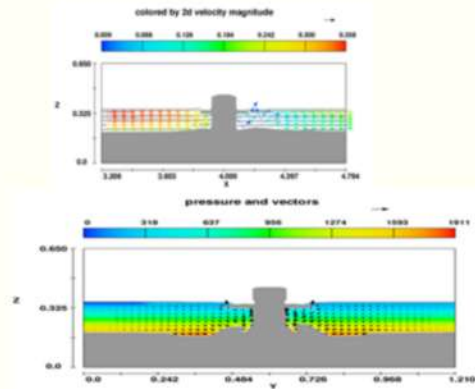


fig 30: Reduction of scouring after adding collar and velocity profile

When a collar is attached to the pier, the scouring starts from the back of the pier due to the effect of wake vortex and horseshoe vortex. The scour hole very gradually develops toward upstream and undermines the collar. After the collar is undermined, the scouring accelerates again. Scour depth of single pier during the experiment is greater than the pier protected with collar, since the collar causes down flow loses its strength on excavating the bed. For single pier, since the down-flow at upstream of the pier is impinging the bed, the scouring process starts rapidly. For pier protected with collar, direct action of down-flow is blocked therefore the scouring starts with delay. After the scouring starts the horseshoe vortex commences to dominate the scouring process. As the scour hole develops, the horseshoe vortex grows in both size and strength. The rate of scouring in this stage is considerably less than that of the initial stage. A collar prevents the direct impact of down flow and decreases the local scour depth by reducing the strength of the down flow and the horseshoe vortex, hence scouring is postponed.



## 5. SUMMARY AND CONCLUSIONS

We have found our desirable scouring depth by addressing collar around the circular shaped piers. In piers protected with collar, at the beginning of the test, wake vortices sweep up the sediments in downstream of the pier in contrast to the unprotected pier in which scouring starts in upstream of the pier due to the effect of the down flow. Two grooves gradually develop at the downstream rim of the collar, and extend towards upstream and eventually reach at upstream edge of the collar. At this moment, the flow is intensified through the grooves, reducing the side slope of the grooves and with sediment removal from the grooves the scour hole extends to upstream of the pier and below the collar.

Now if we look at our second purpose of study is to know which structure is more suitable to select as the pillar structure. From the above comparison between five geometrical structures it is very clear that the lowest maximum scour depth has been observed in case of circular shape pier. And the result of maximum scour depth for the rest of the geometry is not satisfactory that can help us to reduce the scouring around bridge piers. So the current circular shape pier which has been used worldwide for so many years is the best one according to our study.

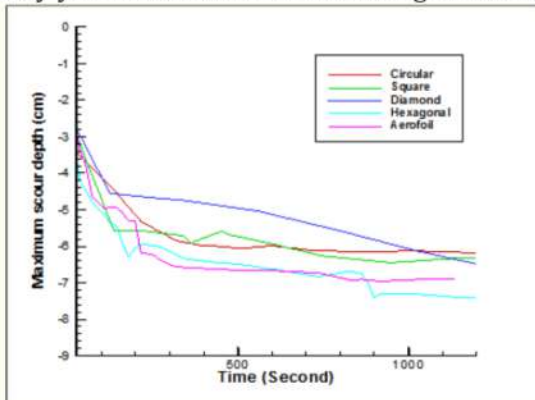


Fig 31: Comparison of maximum scour depth among five piers structures

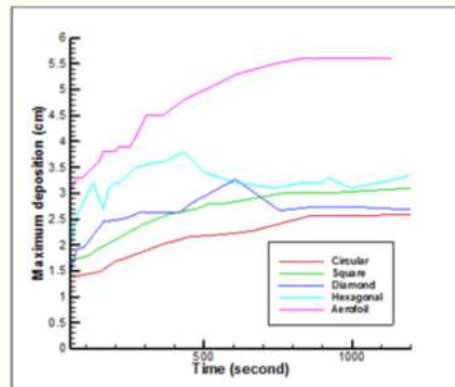


Fig 32: Comparison of maximum deposition among five piers structures

Shape of Bridge Piers	Maximum Scour Depth(Numerical)	Maximum Scour Depth (Experimental)
Circular	6.5cm	6.7cm
Square	6.6cm	7.6cm
Diamond	8.5cm	8.3cm

Table 4: Numerical and experimental maximum scour depths for circular, square and diamond pier

Shape of Bridge Piers	Maximum Deposition (Numerical)	Maximum Deposition (Experimental)
Circular	2.6cm	4.1cm
Square	2.9cm	5.5cm
Diamond	4.8cm	5.5cm

Table 6: Numerical and experimental maximum deposition heights for circular, square and diamond pier

Shape of Bridge Pier	Scour Depth	Deposition of Sand
Hexagonal	8.0cm	3.9cm
<u>Aerofoil</u>	7.9cm	3.8cm

Table 7: Numerical maximum scour depth(cm) and maximum deposition heights(cm) for hexagonal and aerofoil pier

Shape of the pier	Percentage
Circular	2.98%
Square	13.15%
Diamond	2.40%

Table 5: Comparison between experimental and numerical result for maximum scour depth

We can show another comparison among the rest four shapes by considering the circular pier as the best one.

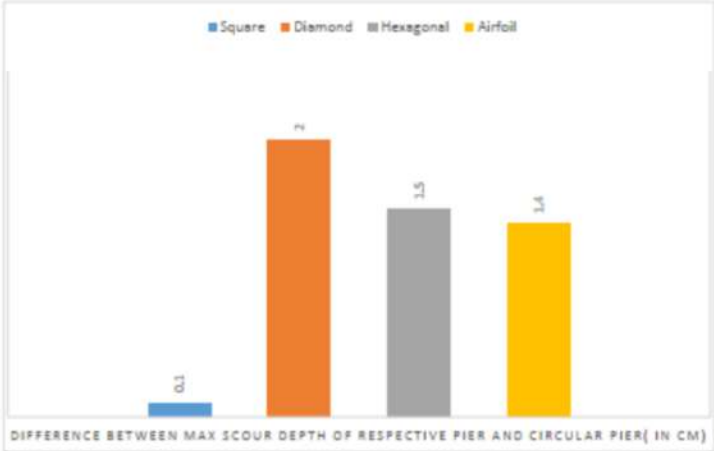


Fig 33: Comparison among square, diamond, hexagonal and airfoil piers

## References

- [1] J. Briaud, F. Ting, H. Chen, R. Gudavalli, S. Perugu and G. Wei, "SRICOS: Prediction of Scour Rate in Cohesive Soils at Bridge Piers", *Journal of Geotechnical and Geoenvironmental Engineering*, vol. 125, no. 4, pp. 237-246, 1999. Available: 10.1061/(asce)1090-0241(1999)125:4(237)
- [2] C. Baker, "The turbulent horseshoe vortex", *Journal of Wind Engineering and Industrial Aerodynamics*, vol. 6, no. 1-2, pp. 9-23, 1980. Available: 10.1016/0167-6105(80)90018-5
- [3] Devenport WJ, Simpson RL. Time-dependent and time-averaged turbulence structure near the nose of a wing-body junction. *J Fluid Mech* 1990;210(2):23–55.
- [4] J. Agui and J. Andreopoulos, "Experimental Investigation of a Three-Dimensional Boundary Layer Flow in the Vicinity of an Upright Wall Mounted Cylinder (Data Bank Contribution)", *Journal of Fluids Engineering*, vol. 114, no. 4, pp. 566-576, 1992. Available: 10.1115/1.2910069.
- [5] Doligalski TL, Smith CR, Walker JDA. Vortex interactions with walls. *Ann Rev Fluid Mech* 1994;26:573–616.
- [6] Seal CV, Smith CR. Visualization of a mechanism for three-dimensional interaction and near-wall eruption. *J Fluid Mech* 1999;394:193–203.

- [7] Martinuzzi R, Tropea C. The flow around surface-mounted, prismatic obstacles placed in a fully developed channel flow. *J Fluids Eng* 1993;115:85–92.
- [8] Hussein H, Martinuzzi R. Energy balance for turbulent flow around a surface mounted cube placed in a channel. *Phys Fluids* 1996;8:764–80.
- [9] Unger J, Hager WH. Down-flow and horseshoe vortex characteristics of sediment embedded bridge piers. *Exp Fluids* 2007;42(1):119.
- [10] Mendoza-Cabrales C. Computation of flow past a cylinder mounted on a flat plate. In: *ASCE Hydraulic engineering, proceedings of national conference*.
- [11] Richardson JE, Panchang VG. Three-dimensional simulation of scour-inducing flow at bridge piers. *J HydraulEng* 1998;124(5):530–40.
- [12] Tseng MH, Yen CL, Song CCS. Computation of three-dimensional flow around square and circular piers. *Int J Numer Methods Fluids* 2000;34:207–27.
- [13] NurtjahyoPY. Numerical Simulation of Pier Scour and Contraction Scour, Ph.D. thesis, Department of Civil Engineering, Texas A&M University, Texas; 2002.
- [14] Ge L, Sotiropoulos F. 3d unsteady RANS modeling of complex hydraulic engineering flows. part I: Numerical model. *J HydraulEng* 2005;131(9):800–8.

- [15] Salaheldin TM, Imran J, Chaudhry MH. Numerical modeling of three-dimensional flow field around circular piers. *J HydraulEng* 2004; 130(2):91100.
- [16] <https://www.usgs.gov/media/images/scour-hole-around-bridge-pier>
- [17] *Jbatrust.org*, 2020. [Online]. Available: <https://www.jbatrust.org/wp-content/uploads/2016/01/JBA-Trust-Flood-and-scour-failure-at-railway-assets-1846-to-2013-W13-4224-FINAL.pdf>.
- [18] Shirhole, A. M., and Holt, R. C. "Planning for a comprehensive bridge safety program." *Transportation Research Record No. 1290*, Transportation Research Board, National Research Council, Washington, D.C. 1991
- [19] Lagasse, P. F., Richardson, E. V., Schall, J. D., and Price, G. R. "Instrumentation for measuring scour at bridge piers and abutments." *National Cooperative Highway Research Program (NCHRP) Report No. 396*, Transportation Research Board, Washington, D.C 1997
- [20] Alabi, P.D. Time development of local scour at bridge pier fitted with a collar. Master Science Thesis, University of Saskatchewan, Canada 2006
- [21] Briaud, J.L., Gardoni, P., Yao, C. . Bridge Scour Risk, ICSE6 Paris. ICSE6-011 -2012

- [22] K. Subramanya, *Flow in open channels*, 3rd ed. New Delhi: McGraw Hill Education (India), 2015, pp. 483-485.
- [23] "Bridge scour", *En.wikipedia.org*, 2020. [Online]. Available: [https://en.wikipedia.org/wiki/Bridge\\_scour](https://en.wikipedia.org/wiki/Bridge_scour).
- [24] B. Melville and S. Coleman, *Bridge scour*. 2000.
- [25] G. Wei, J. Brethour, M. Grünzner and J. Burnham, "Sedimentation Scour Model", *Flow Science Report 03-14*, 2014.
- [26] A. Khosronejad, S. Kang and F. Sotiropoulos, "Experimental and computational investigation of local scour around bridge piers", *Advances in Water Resources*, vol. 37, pp. 73-85, 2012. Available: 10.1016/j.advwatres.2011.09.013.
- [27] Melville BW, ChiewYM. Time scale for local scour at bridge piers. *J HydraulEng* 1999;125(1):59–65.
- [28] Dargahi B. Controlling mechanism of local scouring. *J HydraulEng* 1990;116(10):1197–214.

- [29] Roulund A, Sumer BM, Fredsoe J, Michelsen J. Numerical and experimental investigation of flow and scour around a circular pile. *J Fluid Mech* 2005;534:351–401.
- [30] Ram, S. "A Theoretical Model to Predict Local Scour at Bridge Piers in Non-cohesive Soils." *Proc., River Sedimentation Theory and Application*, A.A. Balkema, Rotterdam, Brook Field, 173-178, 1999
- [31] Melville, B.W. and Chiew, Y.M. . "Time Scale of Local Scour around Bridge Piers." *J. of Hydraulic Engineering*. ASCE, 125(1), 59-65, 1999
- [32] Kothiyari, U.C., Garde, R.C.J., and Raju, K.G.R. (1992a). "Temporal Variation of Scour around Circular Bridge Piers." *J. of Hydraulic Engineering*, ASCE, 118(8), 1091-1105.
- [33] Johnson, P.A. and Bilal, M.A. "Assessing Time Variant Bridge Reliability due to Pier Scour." *J. of Hydraulic Engineering*, ASCE, 118(6), 887-903, 1992
- [34] Laursen, E.M. "An Analysis of Relief Bridge Scour." *J. of Hydraulic Engineering*, ASCE, 89(3), 93-118, 1963
- [35] Vittal, N., Kothiyari, V.c. and Haghghat, M. "Clear Water Scour around Bridge Pier Group." *J. of Hydraulic Engineering*, ASCE, 120(11), 1309-1318, 1994



- [36] Jain, S.c. and Fischer, E.E. "Scour around Bridge Piers at High Flow Velocities." *J. of Hydraulic Engineering*, ASCE, 106(11), 1827-1842,1981
- [37] Kothiyari, U.c., Garde, R.C.J. and Raju, K.G.R. (1992b). "Live Bed Scour around Cylindrical Bridge Piers." *Journal of Hydraulic Research*, IAHR, 30 (5),701 715.
- [38] Laursen, E.M. "Scour at Bridge Crossings." *Trans.*, 127(I), ASCE, Paper 3294,1962
- [39] Molinas, A. and Abdeldayem, A. "Effect of Clay Content on Bridge Scour." *J. of Water Resources Engineering*, ASCE, 1,280-285,1998
- [40] Raudkivi, A.J. and Ettema, R. "Effects of Sediment Gradation on Clear Water Scour." *J. of Hydraulic Engineering*, ASCE, 103(10), 1209-1212,1977